Photoluminescence of rare-earth ion (Eu^{3+}, Tm^{3+}, and Er^{3+})-doped and co-doped $ZnNb_2O_6$ for solar cells*

Gao Sen-Pei(高森沛)[a)b)], Qian Yan-Nan(钱艳楠)[c)], and Wang Biao(王 彪)[a)b)†]

[a)] State Key Laboratory of Optoelectronic Materials and Technologies, Sun Yat-Sen University, Guangzhou 510275, China
[b)] School of Physics and Engineering, Sun Yat-Sen University, Guangzhou 510275, China
[c)] School of Materials and Energy, Guangdong University of Technology, Guangzhou 510275, China

(Received 21 January 2015; revised manuscript received 17 March 2015; published online 20 June 2015)

Visible converted emissions produced at an excitation of 286 nm in $ZnNb_2O_6$ ceramics doped with rare-earth ions (*RE* = Eu^{3+}, Tm^{3+}, Er^{3+} or a combination of these ions) were investigated with the aim of increasing the photovoltaic efficiency of solar cells. The structure of *RE*:$ZnNb_2O_6$ ceramics was confirmed by x-ray diffraction patterns. The undoped $ZnNb_2O_6$ could emit a blue emission under 286-nm excitation, which is attributed to the self-trapped excitons' recombination of the efficient luminescence centers of edge-shared NbO_6 groups. Upon 286-nm excitation, Eu:$ZnNb_2O_6$, Tm:$ZnNb_2O_6$, and Er:$ZnNb_2O_6$ ceramics showed blue, green, and red emissions, which correspond to the transitions of $^5D_0 \rightarrow {}^7F_J$ (J = 1–4) (Eu^{3+}), $^1G_4 \rightarrow {}^3H_6$ (Tm^{3+}), and $^2H_{11/2}/{}^4S_{3/2} \rightarrow {}^4I_{15/2}$ (Er^{3+}), respectively. The calculated CIE chromaticity coordinates of Eu:$ZnNb_2O_6$, Tm:$ZnNb_2O_6$, and Er:$ZnNb_2O_6$ are (0.50, 0.31), (0.14, 0.19), and (0.29, 0.56), respectively. *RE* ion-co-doped $ZnNb_2O_6$ showed a combination of characteristic emissions. The chromaticity coordinates of Eu/Tm:$ZnNb_2O_6$, Eu/Er:$ZnNb_2O_6$, and Tm/Er:$ZnNb_2O_6$ were calculated to be (0.29, 0.24), (0.45, 0.37), and (0.17, 0.25).

Keywords: *RE*:$ZnNb_2O_6$, photoluminescence, solar cell

PACS: 78.55.–m, 81.05.Je, 42.70.–a **DOI:** 10.1088/1674-1056/24/8/087803

1. Introduction

Rare-earth ion-doped materials, which are used as light converter layers for enhancing the photovoltaic efficiency of solar cells, are currently attracting extensive interest.[1–3] Although these solar cells could fill the energy gap left by fossil fuels, the transmission of sub-bandgap light still limits the photovoltaic efficiency of solar cells. In particular, the dye-sensitized solar cell only has high absorption in the visible range of 400 nm–700 nm, due to its wide bandgap of about 1.7 eV–1.8 eV.[4] Therefore, many researchers have sought to expand the possibilities for light converter layers that can convert the ultra-violet (UV, $\lambda < 400$ nm) into the visible emissions.[5–8]

There are many studies on host materials, such as nanosystems, glass-systems, polymer-systems, and others. However, it is worthwhile to study the optical characteristics of rare-earth ion-doped zinc niobate ($ZnNb_2O_6$, ZN) because ZN ceramic is an interesting photoactive material and a typical dielectric material. $ZnNb_2O_6$ ceramic, which has an orthorhombic Columbite structure, exhibits excellent dielectric properties at microwave frequencies with a high dielectric constant ($\varepsilon_r = 25$), high quality factor ($Q \times f = 83700$ GHz), and low temperature coefficient of resonant frequency ($\tau_f = -56$ ppm/°C).[9] Furthermore, $ZnNb_2O_6$ also displays good magnetic, catalytic, and optical properties.[10] Driven by the need for integration of tiny optoelectronic devices, the rare-earth ion-doped $ZnNb_2O_6$ (*RE*:$ZnNb_2O_6$) ceramics could be expanded since *RE*:$ZnNb_2O_6$ has possibilities to combine the dielectric and photoluminescence properties of $ZnNb_2O_6$ with the optical characteristics presented by rare-earth ions. Zhou *et al.*[11] first reported that in rare-earth-doped $ZnNb_2O_6$, the concentration of doped Dy^{3+} ions could influence the intensity of blue emission originating from pure $ZnNb_2O_6$ by energy transfer between Dy^{3+} and niobate groups. Gou *et al.*[12] discovered a shift of chromaticity coordinates from the cold-white region of Dy^{3+}:$ZnNb_2O_6$ to the warm-white region of Dy^{3+}/Al^{3+}:$ZnNb_2O_6$ phosphor under 365-nm excitation. Hsiao *et al.*[13] reported red emission of Eu:$ZnNb_2O_6$ under 288-nm excitation and blue emission of Tm:$ZnNb_2O_6$ under 282-nm excitation, both of which have potential applications in solar cells. Wang *et al.*[14] prepared Ho^{3+}/Yb^{3+}:$ZnNb_2O_6$ ceramics by a high temperature solid state method and reported green and red upconversion emissions in Ho^{3+}/Yb^{3+}:$ZnNb_2O_6$ under 980-nm excitation. Therefore, studying the optical characteristics of *RE*:$ZnNb_2O_6$ ceramics is worthwhile because they can increase the solar spectrum response of dye-sensitized solar cells.

In the present paper, we report how RE ion-doped and -co-doped $ZnNb_2O_6$ ceramics were successfully synthesized by a high temperature solid state method. The structural properties of *RE*:$ZnNb_2O_6$ were evaluated by x-ray diffraction

*Project supported by the National Natural Science Foundation of China (Grant Nos. 10572155 and 10732100) and the Research Fund for the Doctoral Program of Ministry of Education, China (Grant No. 20130171130003).

†Corresponding author. E-mail: wangbiao@mail.sysu.edu.cn

© 2015 Chinese Physical Society and IOP Publishing Ltd

(XRD) patterns. The excitation and emission spectra of the prepared *RE*:$ZnNb_2O_6$ ceramics were investigated under 286-nm excitation. The CIE chromaticity coordinates for the fluorescence of *RE*:$ZnNb_2O_6$ ceramics were calculated based on the 1931 CIE standard and marked in the CIE standard chromaticity diagram.

2. Experiment

A series of RE ion-doped and -co-doped $ZnNb_2O_6$ ceramics were prepared by a high temperature solid state method. The concentrations of Eu^{3+}, Tm^{3+}, and Er^{3+} ions in ZN ceramics are shown in Table 1. The detailed procedure was as follows. The purities of the raw materials (Eu_2O_3, Tm_2O_3, Er_2O_3, ZnO, and Nb_2O_5) were 99.99%. The raw materials, which had been precisely weighed and thoroughly mixed for 24 hours, were fully ground in an agate mortar for 3 hours and then pressed into tablets. The tablets were sintered 2 h at 500 °C and 800 °C and then 4 h at 1150 °C, to get the phase-pure rare-earth-doped $ZnNb_2O_6$ ceramics. The structure of *RE*:$ZnNb_2O_6$ ceramics was identified by x-ray diffraction (XRD) using a Rigaku D-Max 2200PC diffractometer with Cu-Kα radiation ($\lambda = 0.15418$ nm). A combined fluorescence lifetime and steady state spectrometer, FLSP920 by Edinburgh Instruments Ltd., was used to measure the excitation and emission spectra. All of these measures were performed at room temperature.

Table 1. Raw material compositions (mol %) of RE ions in ZN ceramics.

Samples	Concentration/(mol%)		
	Eu^{3+}	Tm^{3+}	Er^{3+}
ZN	0	0	0
Eu:ZN	2	0	0
Tm:Zn	0	2	0
Er:ZN	0	0	2
Eu/Tm:ZN	1	1	0
Eu/Er:ZN	1	0	1
Tm/Er:ZN	0	1	1

3. Results and discussion

The powder XRD patterns of pure and *RE*:$ZnNb_2O_6$ ceramics are shown in Fig. 1. The result shows that all of the diffraction peaks can be well indexed to the known phase of $ZnNb_2O_6$ based on the standard XRD pattern (JCPDS#37-1371). No new peaks appear in the XRD pattern of *RE*:$ZnNb_2O_6$ compared with the undoped $ZnNb_2O_6$ ceramic, indicating that the doping ions (Eu^{3+}, Tm^{3+}, and Er^{3+}) have no influence on the structure of *RE*:$ZnNb_2O_6$, and *RE*:$ZnNb_2O_6$ is still an orthorhombic system. So it is speculated that the doping Eu^{3+}, Tm^{3+}, and Er^{3+} ions may occupy the normal Zn-site or Nb-site rather than interstitial sites of the lattice.

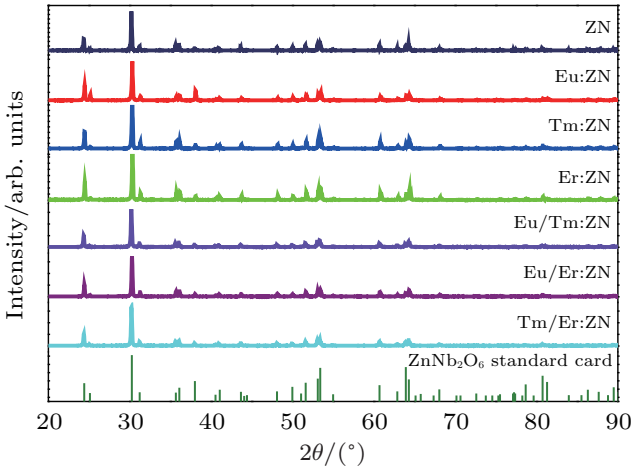


Fig. 1. (color online) XRD patterns of prepared $ZnNb_2O_6$ ceramics.

$ZnNb_2O_6$ has been investigated as a self-activated blue phosphor,[15] figure 2 shows the excitation and emission spectra of the pure $ZnNb_2O_6$ ceramic with monitoring excitation at 286 nm and emission at 470 nm. The broad excitation band showed absorption within the range from 230 nm to 310 nm. A blue emission band centered at 470 nm is observed in the self-activated $ZnNb_2O_6$ ceramic under 286-nm excitation. It is known that in the orthorhombic columbite structure of $ZnNb_2O_6$, both Zn and Nb atoms, which are centered at the octahedron, are surrounded by six O^{2-} anions to form ZnO_6 and NbO_6 octahedra, respectively. The octahedra are connected to each other via sharing edge or corner to form a two-dimensionally extended sheet in the *bc* plane.[16] Here, the edge-sharing $[NbO_6]^{7-}$ groups are efficient luminescent centers for blue emission,[17] which may be ascribed to recombination of self-trapped excitons.[18] Fragoso *et al.*[19] also reported that edge-sharing NbO_6 octahedral groups show efficient blue luminescence with a large Stokes shift. As illustrated in Fig. 2, the observed emission bands at 445 nm, 615 nm, and 659 nm can be attributed to the defects and impurities generated from extrinsic niobate groups.[20]

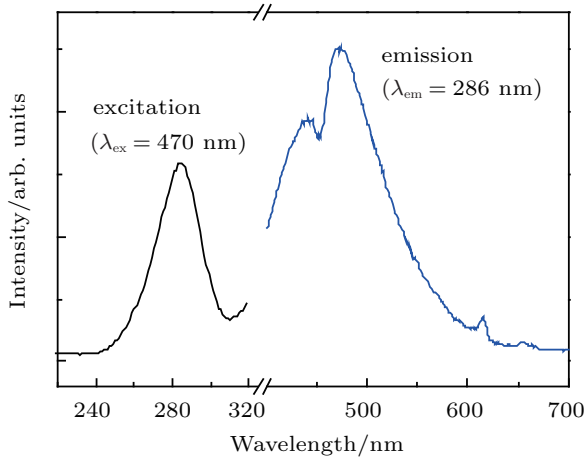


Fig. 2. (color online) Excitation and emission spectra of undoped $ZnNb_2O_6$.

Figure 3(a) shows the excitation spectrum (λ_{em} = 615 nm) of Eu:ZN and the corresponding emission spectra (λ_{ex} = 286 nm) of Eu:ZN. The inset of Fig. 3(a) shows the emission color of Eu:ZN under 286-nm excitation, and a bright red-light emission in Eu:ZN ceramic can be easily observed by the naked eye. It can be clearly observed that the excitation spectrum consists of two main features, a strong broad band centered at 286 nm and a weak one at 396 nm. The 286-nm excitation band corresponds to the charge transfer from the 2p orbitals of the O^{2-} to the 5d orbitals of the central Nb^{5+} atoms in the $[NbO_6]^{7-}$ groups. The presence of the 286-nm excitation peak indicates that there is an energy transfer from the $[NbO_6]^{7-}$ groups to Eu^{3+} in Eu:ZN. The excitation band at 396 nm, which belongs to the characteristic f–f transition lines within the $^4f_6$ configuration of the Eu^{3+} ion, is assigned to the $^7F_0 \rightarrow {}^3L_6$ transition of Eu^{3+} ion. Under 286-nm excitation, the observed visible emissions are centered at 595 nm, 615 nm, 628 nm, and 655 nm, as shown in the right of Fig. 3(a), and are attributed to the typical transitions of $^5D_0 \rightarrow {}^7F_J$ (J = 1–4), respectively. The green emission at 540 nm corresponds to the transition of $^5D_1 \rightarrow {}^7F_1$ of Eu^{3+} ions in the Eu:ZN ceramic. Hsiao *et al.*[13] also reported the red emission at 613 nm of Eu^{3+} ion-doped $ZnNb_2O_6$ under 288-nm excitation due to the $^5D_0 \rightarrow {}^7F_2$ transition of Eu^{3+}. In addition, they reported the influence of the concentration of Eu^{3+} on the emission intensity of Eu^{3+} ion-doped $ZnNb_2O_6$.

The photoluminescence excitation (λ_{em} = 484 nm) and emission (λ_{ex} = 286 nm and 362 nm) spectra of Tm:ZN are displayed in Fig. 3(b). It can be seen that the 286-nm and 362-nm excitation bands appear in the excitation spectrum of Tm:ZN. Similar to the Eu:ZN ceramic, the 286-nm excitation band is due to the 2p(O)–4d(Nb) charge transfer transitions. The strong narrow line at 362 nm can be ascribed to the characteristic f–f transition ($^3H_6 \rightarrow {}^1D_2$) of Tm^{3+} within its $4f^{12}$ configuration. The inset of Fig. 3(b) shows that Tm:ZN ceramic could emit a bright blue-light emission, which can be easily observed by the naked eye. As illustrated in the emission spectrum of Tm:ZN under 286-nm excitation, a strong emission at 484 nm corresponds to the $^1G_4 \rightarrow {}^3H_6$ transition of Tm^{3+} ions. The two weak emissions observed at 460 nm and 655 nm are due to the $^1D_2 \rightarrow {}^3F_4$ and $^1G_4 \rightarrow {}^3F_4$ transitions, respectively. Hsiao *et al.*[13] reported that the concentration of Tm^{3+} influences the blue emission intensity of Tm:$ZnNb_2O_6$. We both converted UV light into visible emission in RE-doped $ZnNb_2O_6$. Following 362-nm excitation at room temperature, the typical emission spectrum of Tm:ZN shows an intense emission at around 460 nm, which corresponds to the intra 4f–4f $^1D_2 \rightarrow {}^3F_4$ electronic transition of Tm^{3+} ions.

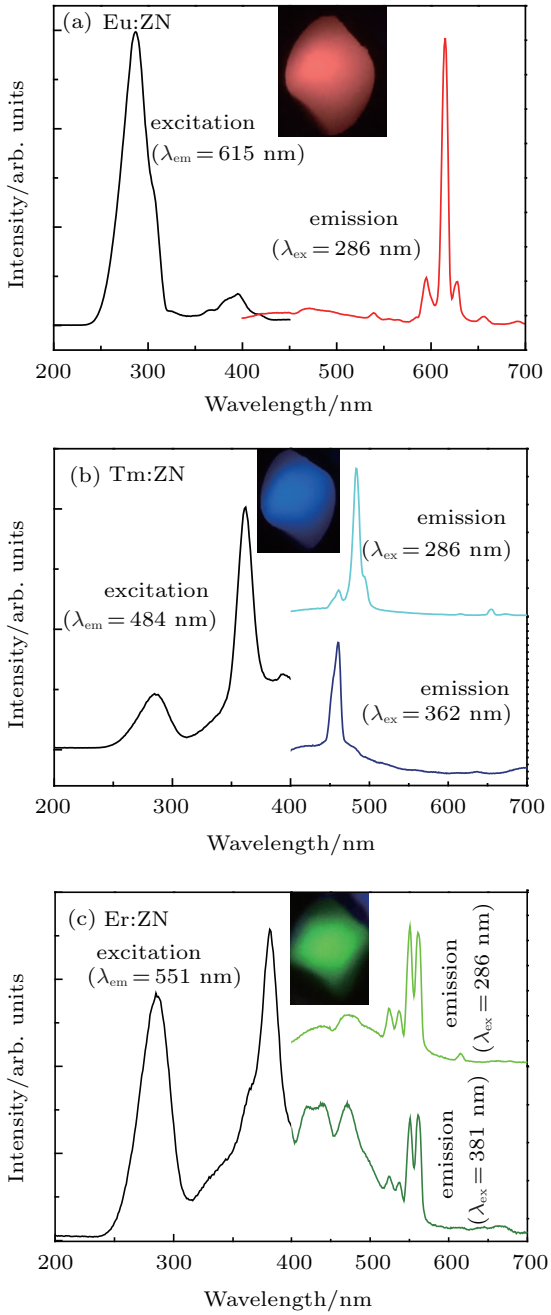


Fig. 3. (color online) Excitation and emission spectra of (a) Eu:ZN, (b) Tm:ZN, and (c) Er:ZN.

Figure 3(c) is the excitation spectrum of Er:ZN that is obtained by monitoring the emission at 552 nm and the emission spectra (λ_{ex} = 286 nm and 381 nm) of Er:ZN. It can be clearly seen from the excitation spectrum of Er:ZN that two broad excitation bands are centered at 286 nm and 381 nm, respectively. The charge transfer from the 2p orbitals of the O^{2-} to the 5d orbitals of the Nb^{5+} contributes to the 286-nm excitation peak in the excitation spectrum of Er:ZN. The strong narrow line at 381 nm is assigned to the $^4I_{15/2} \rightarrow {}^4G_{11/2}$ transition of Er^{3+} ion. It can be seen from the inset of Fig. 3(c) that the emission color of Er:ZN looks green to the naked eye. In the emission spectrum of Er:ZN under 286-nm excitation, the green emissions at 524 nm and 550 nm are assigned to the

$^2H_{11/2} \rightarrow {}^4I_{15/2}$ and $^4S_{3/2} \rightarrow {}^4I_{15/2}$ transitions of Er^{3+} ion, respectively. It can also be seen that a blue emission centered at 470 nm is observed in the Er:ZN ceramic. The 470-nm blue emission, illustrated in Fig. 2, is ascribed to the self-activated $ZnNb_2O_6$ host materials. The photoluminescence emission spectrum of Er:ZN upon 381-nm excitation is shown in Fig. 3(c). The observed emissions from 410 nm to 480 nm are attributed to host material, while emissions at 524 nm and 550 nm are due to $^2H_{11/2} \rightarrow {}^4I_{15/2}$ and $^4S_{3/2} \rightarrow {}^4I_{15/2}$ transitions of Er^{3+} ions, respectively.

Figure 4 shows the energy diagram level of Eu^{3+}, Tm^{3+}, and Er^{3+} ions, as well as a simple model illustration of the energy transfers from the NbO_6 groups to the RE ions. Under 286-nm excitation, the ground state of the $[NbO_6]^{7-}$ groups is populated to the excited state, which has a large Stokes shift effect from Nb–O charge transfer. As for Eu:ZN, the excited state of Nb–O bonds can transfer its energy to the $^5D_4$ state of Eu^{3+} ions through energy transfer (ET1: $[NbO_6]^{7-}$ + 286 nm $\rightarrow {}^5D_4$ (Eu^{3+})). Then, the $^5D_0$ and $^5D_1$ states of Eu^{3+} ions are populated via a nonradiative relaxation (NR) process. The Eu^{3+} ions at the $^5D_0$ and $^5D_1$ states give the radiative transitions of $^5D_0 \rightarrow {}^7F_J$ (J = 1–4) and $^5D_1 \rightarrow {}^7F_1$, producing emissions at 595 nm, 615 nm, 628 nm, 655 nm, and 540 nm, respectively.

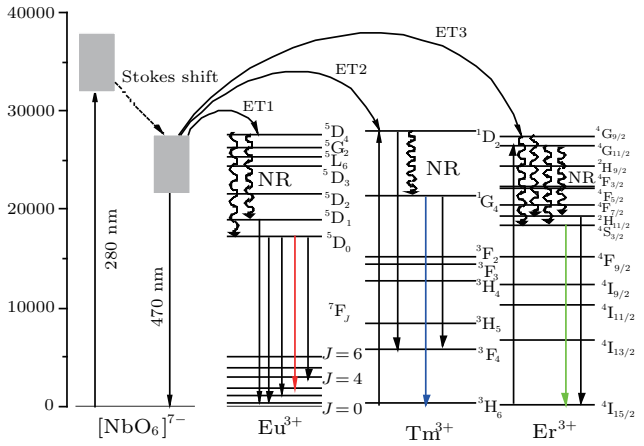


Fig. 4. (color online) The energy diagram level of Eu^{3+}, Tm^{3+}, and Er^{3+} ions, as well as a simple model illustration of the energy transfers from the NbO_6 groups to the RE ions.

In the case of the Tm:ZN ceramic upon excitation of the 286-nm UV light, the $^1D_2$ state of Tm^{3+} can be excited by ET2 process ($[NbO_6]^{7-}$ + 286 nm $\rightarrow {}^1D_2$ (Tm^{3+})). Subsequently, the $^1G_4$ state of Tm^{3+} ions is populated by NR from the $^1D_2$ state. Tm^{3+} ions at the $^1G_4$ state decay radiatively to the $^3H_6$ ground state, resulting in an intense blue emission at 484 nm. Meanwhile, the $^1D_2 \rightarrow {}^3F_4$ and $^1G_4 \rightarrow {}^3F_4$ transitions of Tm^{3+} ions produce 460-nm and 655-nm emissions, respectively. In Tm:ZN, the Tm^{3+} ions in the $^3H_6$ ground state can also be directly excited by 362-nm wavelength light up to the $^1D_2$ state. The Tm^{3+} ions at the $^1D_2$ state radiatively relax to the $^3F_4$ state, generating 460-nm emission.

The energy transfer process between NbO_6 groups and Er^{3+} ions in Er:ZN is similar to those of Eu:ZN and Tm:ZN ceramics, the ET3 process ($[NbO_6]^{7-}$ + 286 nm $\rightarrow {}^4G_{9/2}$ (Er^{3+})) could excite the $^4G_{9/2}$ state of Er^{3+} ions under 286-nm excitation. The Er^{3+} ions at the $^4G_{9/2}$ state nonradiatively relax to the green-emitting $^2H_{11/2}/{}^4S_{3/2}$ states in cascade. The green emissions at 524 nm and 550 nm are produced by the radiative relaxation process from the $^2H_{11/2}/{}^4S_{3/2}$ states to the ground $^4I_{15/2}$ state, respectively. It can also be seen that Er^{3+} ions at the ground $^4I_{15/2}$ state are excited to the $^4G_{11/2}$ state under 381-nm excitation. Then, the green-emitting $^2H_{11/2}/{}^4S_{3/2}$ states are populated by NR process from the $^4G_{11/2}$ state, producing emissions at 524 nm and 550 nm.

The optical characteristics of RE ion-co-doped ZN ceramics have been studied in order to expand the solar spectrum response of dye-sensitized solar cells. Figure 5 shows the emission spectra of Eu^{3+}/Er^{3+}, Eu^{3+}/Tm^{3+}, and Er^{3+}/Tm^{3+} co-doped $ZnNb_2O_6$ ceramics under 286-nm excitation. It can be seen from Fig. 5(a) that there is a blue emission at 460 nm and emissions at 595 nm, 615 nm, 628 nm, and 655 nm, which are ascribed to the $^1G_4 \rightarrow {}^3H_6$ transition of Tm^{3+} ions and $^5D_0 \rightarrow {}^7F_J$ (J = 1–4) transitions of Eu^{3+} ions, respectively. Compared with the emission spectra of Eu:ZN and Tm:ZN ceramics, Eu/Tm:ZN emits a combination of optical characteristics of Eu^{3+} and Tm^{3+} ions, which is beneficial for the efficiency of light-light conversion. The emission spectrum of Eu/Er:ZN (shown in Fig. 5(b)) exhibits a strong red emission at 615 nm, which can be attributed to the $^5D_0 \rightarrow {}^7F_3$ transition of Eu^{3+} ion. The three weak emissions obtained at 595 nm, 628 nm, and 655 nm correspond to $^5D_0 \rightarrow {}^7F_J$ (J = 1, 2, and 4), respectively. The green emissions at 550-nm are assigned to the $^4S_{3/2} \rightarrow {}^4I_{15/2}$ transition of Er^{3+} ions. A strong blue emission at 460 nm, as shown in Fig. 5(c), results from the $^1G_4 \rightarrow {}^3H_6$ transition of Tm^{3+} ions, and the weak green emissions are due to the $^4S_{3/2} \rightarrow {}^4I_{15/2}$ transitions of Er^{3+} ions. The experimental results show that the RE ion-co-doped ZN ceramic successfully combined the optical characteristics of two different RE ions. Seeta Rama Raju *et al.*[21] reported that Tm^{3+}, Eu^{3+}, and Er^{3+} ion-doped and ion-co-doped $BaGd_2O_4$ combined the optical characteristics of different RE ions. Moreover, Tm^{3+}, Eu^{3+}, and Er^{3+} ion-tri-doped $BaGd_2O_4$ also showed the characteristic emissions of Tm^{3+}, Eu^{3+}, and Er^{3+} ions. Usually, the absorption wavelength of a solar cell is about 400 nm–1000 nm. Figures 3 and 5, considered together, show that RE ions-doped and co-doped ZN can efficiently convert UV light into a visible emission. The RE ion-doped and ion-co-doped ZN are considered for use as a downconversion layer placed on the front side of a silicon solar cell, which is combined with a back optical reflector. The *RE*:ZN downconversion layer absorbs UV solar radiation and emits visible emissions that are subsequently reabsorbed by

the dye-sensitized solar cell. Moreover, RE ion-co-doped ZN ceramics can also enlarge the solar spectrum response because they can combine the optical characteristics of two different RE ions.

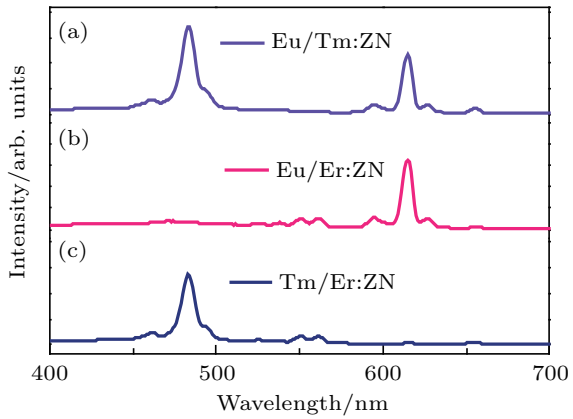


Fig. 5. (color online) The emission spectra of (a) Eu^{3+}/Tm^{3+}:ZN, (b) Eu^{3+}/Er^{3+}:ZN, and (c) Tm^{3+}/Er^{3+}:ZN under 286-nm excitation.

To characterize the true color of emitted light, it is necessary to study the color coordinates marked on a standard chromaticity diagram. The CIE 1931 *xy* chromaticity coordinates of *RE*:ZN (*RE* = Eu^{3+}, Tm^{3+}, and Er^{3+}) under 286/362/381-nm excitation can be calculated by the following formula[22] and are presented in Fig. 6:

$$x = \frac{X}{X+Y+Z};\ y = \frac{Y}{X+Y+Z};\ z = \frac{Z}{X+Y+Z}, \quad (1)$$

where X, Y, and Z are the three tristimulus values, which can be given by[23]

$$X = \int_{400}^{700} P(\lambda)x'(\lambda)\mathrm{d}\lambda, \quad (2)$$

$$Y = \int_{400}^{700} P(\lambda)y'(\lambda)\mathrm{d}\lambda, \quad (3)$$

$$Z = \int_{400}^{700} P(\lambda)z'(\lambda)\mathrm{d}\lambda, \quad (4)$$

where $P(\lambda)$ is the tristimulus value for a color with a spectral power distribution, λ is the wavelength of the equivalent monochromatic light, $x'(\lambda)$, $y'(\lambda)$, and $z'(\lambda)$ are three color-matching functions. According to the above equations, the calculated chromaticity coordinates of *RE*:ZN ceramics are listed in Table 2. As illustrated in Table 2, the chromaticity coordinates of Eu:ZN, Tm:ZN, and Er:ZN are (0.50, 0.31), (0.14, 0.19), and (0.29, 0.56) under 286-nm excitation, which indicate red, blue, and green emissions, corresponding to the colors observed by the naked eye, as shown in Fig. 3. As for the Tm:ZN ceramic under 362-nm excitation, the calculated value of CIE coordinates is (0.22, 0.18), which is located between the blue and purple regions, as shown in Fig. 6. The CIE coordinate for the emission spectrum of Er:ZN under 381-nm excitation is calculated to be (0.30, 0.48), which is located at the region between green and cyan, as shown in Fig. 6. It can be observed from Fig. 6 that the RE-doped ZN under 286-nm excitation has a higher color purity than Tm:ZN under 362-nm excitation and Er:ZN under 381-nm excitation. The color coordinates of RE ion-co-doped ZN ceramics are also listed in Table 2. It can be observed that the calculated coordinates of Eu/Tm:ZN, Eu/Er:ZN, and Tm/Eu:ZN are (0.29, 0.24), (0.45, 0.37), and (0.17, 0.25). It can be seen in Fig. 6 that the CIE coordinates of RE ion-co-doped ZN ceramics are located between the *RE*:ZN under 286-nm excitation, which indicates that multicolor emissions are achieved. Meanwhile, the shift of the CIE chromaticity coordinates confirms that the emission color can be adjusted through co-doping. Thus, we can tune the emission color of *RE*:ZN over a wide range. The obtained visible red, blue, and green emissions of RE ion-doped and ion-co-doped ZN ceramics indicate that *RE*:ZN can be considered to be a promising light converting layer for use in dye-sensitized solar cells.

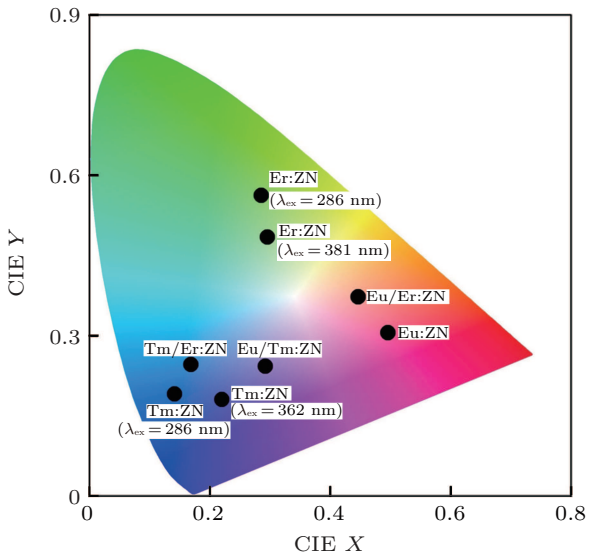


Fig. 6. (color online) CIE chromaticity coordinates of RE-doped and RE-co-doped ZN ceramics.

Table 2. CIE coordinates of *RE*:ZN ceramics.

Samples	CIE (x, y)
Eu:ZN	(0.50, 0.31)
Tm:Zn	(0.14, 0.19) (λ_{ex} = 286 nm) (0.22, 0.18)(λ_{ex} = 362 nm)
Er:ZN	(0.29, 0.56) (λ_{ex} = 286 nm) (0.30, 0.48) (λ_{ex} = 381 nm)
Eu/Tm:ZN	(0.29, 0.24)
Eu/Er:ZN	(0.45, 0.37)
Tm/Er:ZN	(0.17, 0.25)

4. Conclusion

In summary, Eu^{3+}, Tm^{3+}, and Er^{3+} ion-doped and ion-codoped $ZnNb_2O_6$ ceramics have been successfully prepared by a high temperature solid state method. Under 286-nm UV excitation, undoped $ZnNb_2O_6$ shows a blue emission at 470 nm due to the $[NbO_6]^{7-}$ groups. Bright visibly enhanced visible blue, green, and red emissions, induced by 280-nm UV

excitation, are gained in Tm:ZN, Er:ZN, and Eu:ZN ceramics, which can be ascribed to the $^5D_0 \rightarrow {}^7F_J$ ($J = 1$–4) (Eu^{3+}), $^1G_4 \rightarrow {}^3H_6$ (Tm^{3+}), and $^2H_{11/2}/{}^4S_{3/2} \rightarrow {}^4I_{15/2}$ (Er^{3+}), respectively. The emission spectra of RE ion-co-doped $ZnNb_2O_6$ show expanded emission spectra that result from the combination of the emission spectra of the corresponding RE ion-doped $ZnNb_2O_6$. The chromaticity coordinates of *RE*:ZN are calculated and the CIE diagram is presented to demonstrate the change of emission color.

References

[1] Huang X Y, Han S Y, Huang W and Liu X G 2013 *Chem. Soc. Rev.* **42** 173

[2] Chen X B, Li S, Ding X L, Yang X D, Liu Q L, Gao Y, Sun P and Yang G J 2014 *Chin. Phys. B* **23** 087809

[3] Hu Y B, Qiu J B, Zhou D C, Song Z G, Yang Z W, Wang R F, Jiao Q and Zhou D L 2014 *Chin. Phys. B* **23** 024205

[4] Cheng Y Y, Fückel B, MacQueen R W, Khoury T, Clady R G C R, Schulze T F, Ekins-Daukes N J, Crossley M J, Stannowski B, Lips K and Schmidt T W 2012 *Energy Environ. Sci.* **5** 6953

[5] Chen Y C, Huang W Y and Chen T M 2011 *J. Rare Earths* **29** 907

[6] Chen Y, Wang J, Liu C, Tang J, Kuang X, Wu M and Su Q 2013 *Opt. Express* **21** 3161

[7] Wu J, Wang J, Lin J, Xiao Y, Yue G, Huang M, Lan Z, Huang Y, Fan L, Yin S and Sato T 2013 *Sci. Rep.* **3** 2058

[8] Sun J Y, Sun Y N, Zhu J C, Zeng J H and Du H Y 2013 *Chin. Phys. B* **22** 057803

[9] Lee H J, Kim I T and Hong K S 1997 *Jpn. J. Appl. Phys.* **36** 1318

[10] Pullar RC 2009 *J. Am. Ceram. Soc.* **92** 563

[11] Zhou Y, Qiu Z, Lü M, Ma Q, Zhang A, Zhou G, Zhang H and Yang Z 2007 *J. Phys. Chem. C* **111** 10190

[12] Gou J, Wang Y and Guo H 2009 *J. Phys.: Conf. Ser.* **152** 012081

[13] Hsiao Y J, Fang T H and Ji L W 2011 *Mater. Chem. Phys.* **130** 1187

[14] Wang R, Zhang W, Xu Y and Xing L 2014 *Opt. Laser Technol.* **58** 52

[15] Hsiao Y J, Fang T H and Ji L W 2010 *Mater. Lett.* **64** 2563

[16] Ye J H, Zou Z G and Akiyuki M 2003 *Int. J. Hydrogen Energy* **28** 651

[17] Blasse G, Dirksen G J and Brixner L H 1986 *Mater. Chem. Phys.* **14** 485

[18] Srivastava A M and Ackerman J F 1997 *J. Solid State Chem.* **134** 187

[19] Fragoso D, de Mello Donegá C and Longo R L 2003 *J. Lumin.* **105** 97

[20] Zhou Y, Qiu Z, Lv M, Ma Q, Zhang A and Zhou G 2007 *J. Phys. Chem. C* **111** 10190

[21] Seeta Rama Raju G, Pavitra E and Yu J S 2014 *Dalton Trans.* **43** 9766

[22] Ashdown I 2002 *Solid State Lighting II, SPIE* **4776** 51

[23] Mortimer R J and Varley T S 2011 *Displays* **32** 35